Synthesis of Nickel-Zinc Ferrites in RF Thermal Plasma Reactor

J. Szépvölgyi[1,2*], I. Mohai[1], L. Gál[1], I. Mészáros[3], J. Gubicza[4]

[1] Institute of Materials and Environmental Chemistry, Chemical Research Center, Hungarian Academy of Sciences H-1525 POB 17, Budapest, Hungary
[2] Research Institute of Chemical and Process Engineering, University of Pannonia, H-8200 POB 158, Veszprém, Hungary
[3] Research Group for Metals Technology, Hungarian Academy of Sciences and Budapest University of Technology and Economics, H-1521 POB 91, Budapest, Hungary
[4] Department of Solid State Physics, Eötvös University, H-1518 POB 32, Budapest, Hungary

Abstract

Nickel-zinc ferrites usually exhibit high saturation magnetization. They can be used e.g. in ceramic magnetic devices and as carriers for targeted drug release. In this paper results of thermal plasma synthesis of nanosized nickel-zinc ferrites from oxide powders and corresponding nitrate solutions, respectively, are presented. The reaction products were characterized for chemical composition, phase conditions, particle size distribution, morphologies and saturation magnetization. Effect of synthesis conditions on properties of products was studied. Correlations of domain- and particle sizes of nanosized nickel-zinc ferrites were also investigated. It has been proved that in particular conditions complex ferrites of good ferrimagnetic properties could be produced in a single step reaction due to the high reaction temperature and intensive heat and mass transfer conditions.

Keywords: nickel-zinc ferrites, thermal plasma, synthesis

Introduction

Nickel-zinc ferrites are widely used in electromagnetic devices where their favorable properties such as high resistance, high permeability, low eddy current losses and high saturation magnetization can be suitably utilized. Such devices are inductors and electromagnetic wave absorbers [1]. Most applications require sintered ferrites produced from ferrite powders by ceramic technologies. In processing terms ferrite powders of well-defined composition and narrow particle size distribution are preferred.

Nickel-zinc ferrite powders are usually produced by reverse micelle synthesis [2], hydrothermal processing [3], precipitation [4] or intensive ball milling [5].

Another synthesis route involves thermal decomposition of nitrate solutions at high temperatures. First step of the process is the evaporation of the solvent which is followed by the thermal decomposition of nitrates and formation of ferrites [6]. The evaporation, the chemical reaction and the condensation from gas phase take place very rapidly in this case leading to formation of micro- and nanosized particles.

The nickel-zinc ferrites of $Ni_XZn_{(1-X)}Fe_2O_4$ composition belong to the *Fd3m* crystal group and crystallize in face-centered cubic lattice. In normal ferrites the Zn^{2+} and Ni^{2+} cations are located at tetragonal sites while the Fe^{3+} cations occupy the octagonal ones. The oxygen ions are positioned in between. The magnetic momentum of normal nickel-zinc ferrite spinels is zero. Below the Néel temperature they are anti-ferrimagnetic, while above it they are paramagnetic. If we provide sufficient energy to a normal ferrite spinel – by intensive grinding or long-lasting heat treatment – a lattice inversion will occur: certain Fe^{3+} cations will be exchanged by Zn^{2+} and Ni^{2+} cations and *vice versa*. In this way so–called inverse ferrite with composition of $(Fe^{3+}_Y)[Ni^{2+}_X Zn^{2+}_{(1-X)} Fe^{3+}_{2-Y}]O_4$ will form. The inverse ferrites are meta-stable species in thermodynamic terms. The smaller the particle size the easier the formation of inverse structure. The inverse nickel-zinc ferrite spinel is ferrimagnetic material.

It is known that materials of special composition and morphology can produced in thermal plasma conditions. In these systems the reaction temperature is very high, the precursors are heated very rapidly and the products are cooled with a high rate.

In this paper synthesis of inverse nickel-zinc ferrite spinels from different precursors in thermal plasma conditions is discussed. Special attention is devoted to the correlations among the synthesis conditions and properties of products.

Experimental

The experiments were performed in a radiofrequency thermal plasma reactor operating with a TEKNA PL-35 induction plasma torch at a maximum plate power of 30 kW [7]. Argon was used as plasma gas with a flow rate of 20 $l \cdot min^{-1}$. The sheath gas was a mixture of Ar and O_2 with flow rates of 23 $l \cdot min^{-1}$ and 20 $l \cdot min^{-1}$, respectively.

The nickel-zinc ferrite powders were synthesized from the following precursors:

- mixture of NiO, ZnO and Fe_2O_3 powders having particle size of few micrometers;
- ethanol solutions of $Ni(NO_3)_2.6H_2O$, $Zn(NO_3)_2 \cdot 6H_2O$ and $Fe(NO_3)_3 \cdot 9H_2O$; the salt concentration in all cases was 0.65 $mol \cdot dm^{-3}$.

The analytical grade nitrates were dissolved in technical grade ethanol using a magnetic stirrer.

The oxide mixtures were injected into the plasma flame by a PRAXAIR powder feeder, while the nitrate solutions by a TEKNA suspension feeder. The injected precursors were atomized by argon gas with a flow rate of 3 $l \cdot min^{-1}$

along the centerline of the torch. The following synthesis parameters were varied in this work:

- composition of precursors,
- feed rate of precursors and
- plate power of the RF generator.

The reaction products were collected from the water-cooled reactor wall. Their chemical composition was analyzed by ICP-OES (Thermo Jarrell Ash Atomscan 25). A Philips Xpert XRD apparatus operating with Cu K_α radiation was used to analyze the phase composition. The particle size distribution was measured by laser-diffraction method with a Malvern Mastersizer 2000 system. Morphology of products was studied by SEM (Philips XL30 ESEM) and TEM (Philips CM20). The Ni, Zn and Fe content of individual particles was determined by energy dispersive X-ray fluorescence spectroscopy (EDS; NORAN EDS system).

A specially designed vibrating sample magnetometer (VSM) was applied for measuring the first magnetization curves of ferrite powders. Operation of VSM is based on the following principle: if a material is placed into a magnetic field, a dipole moment proportional to its susceptibility and the applied magnetic field will be induced. In case of sinusoid vibration, the resulting magnetic flux induces an electrical signal in the detector coils around the sample. The induced voltage is proportional to the magnetic moment of the sample, the amplitude and the frequency of vibration. Using a vibration controlled reference coil, the amplitude and frequency dependence can be eliminated and the instrument can be calibrated.

The VSM instrument was designed at the Department of Materials Science and Engineering of BME. In contrast to the traditional Foner-type magnetometers, in this VSM instrument the specimen vibrates along the external magnetic field. Therefore, it is called parallel motion vibrating sample magnetometer (PMVSM). This arrangement has several advantages like increased sensitivity, better signal-to-noise ratio, simpler detector coil arrangement and easier positioning of specimens.

In PMVSM the vibration is driven by a sinusoidal signal with a frequency of 75 Hz. A nickel sphere is used as calibration standard. For the ferrite samples a cylindrical specimen holder was designed.

The initial magnetization curves were measured by magnetizing the samples with an external field of about 5000 A/cm. The complete magnetic saturation could be achieved at about 2000 A/cm. The specimens contained both paramagnetic and ferrimagnetic phases in significant amounts. Contribution of the paramagnetic phase was removed from the magnetization curves. Thus, the actual specific saturation magnetization of ferrimagnetic phase was determined [8].

Results and discussion

The experimental conditions and properties of products are summarized in Table 1. Much higher and more uniform feed rates were achieved with nitrate solutions, than with oxide mixtures. Thus, the specific energies defined as the plate power of RF generator related to feed rate of solid precursors were much lower nitrate solutions than for oxide mixtures. The specific energy can be regarded as a parameter characterizing plate power and feed rate of precursors simultaneously.

Table 1 Results of thermal plasma synthesis of nickel-zinc ferrites

Precursor	$NiO + ZnO + Fe_2O_3$			$Ni(NO_3)_2{\cdot}6H_2O+Zn(NO_3)_2{\cdot}6H_2O+Fe(NO_3)_3{\cdot}9H_2O$					
Run No.	NZP1	NZP2	NZP3	NZS1	NZS2	NZS3	NZS4	NZS5	NZS6
Initial Ni:Zn:Fe molar ratio	3:1:2	1:1:2	1:3:2	3:1:2	1:1:2	1:3:2	3:1:2	1:1:2	1:3:2
Experimental conditions									
Position of feeding probe[1]	20	20	20	20	20	20	80	80	80
Plate power (kW)	25	25	25	15	15	15	25	25	25
Feed rate of precursors ($g{\cdot}h^{-1}$)	6	4	15	327	271	345	97	97	97
Specific energy ($kWh{\cdot}g^{-1}$)	4.08	5.73	1.66	0.046	0.055	0.044	0.25	0.25	0.25
Properties of products									
d_{50}(l) (nm)	119	63	274	201	243	244	74	182	214
Magnetite content (m %)	< 1								
Saturation magnetization ($emu{\cdot}g^{-1}$)	35	40	50	34	42	45	38	52	48
Domain size of ferrites (nm)	24	28	50	19	18	20	34	30	36

[1] distance downwards the upper level of induction coil (mm)

Chemical compositions measured by ICP-OES were not listed in Table 1: all products had targeted composition within limits of experimental errors.

In all cases nanosized nickel-zinc ferrites were formed. The characteristic particle size of ferrites is plotted against the composition of precursors (the Ni : Zn molar ratio) and the specific energy in Fig. 1. The d_{50}(l) values are slightly changing against the Ni : Zn molar ratio, while against specific energy they have a rather well-defined maximum. It can be explained by the thermal history of species in the plasma flame region. However, further measurements are required to interpret this phenomenon more precisely.

SEM micrograph of powder NZP1 (Fig. 2) confirms formation of rather uniform, nanosized particles. Increasing resolution (Fig. 3) clearly shows presence of nanosized hexagonal ferrite crystallites.

The saturation magnetization is sensitive to the composition of precursor and the specific energy, as well. The maximum saturation magnetization of about 50 $emu{\cdot}g^{-1}$ was obtained at a Ni : Zn : Fe molar ratio of 1 : 1 : 2 and at specific energy of 2-3 $kWh{\cdot}g^{-1}$ (Fig. 4). Such a value

is not typical for normal Ni-Zn ferrites; it refers to formation of inverse Ni-Zn ferrites.

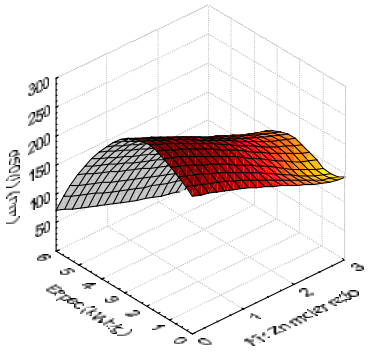

Fig. 1 d_{50}(l) as plotted against Ni:Zn molar ratio and specific energy

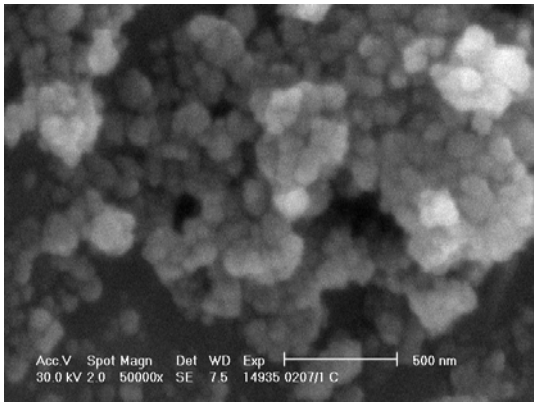

Fig. 2 SEM micrograph of product NZP1

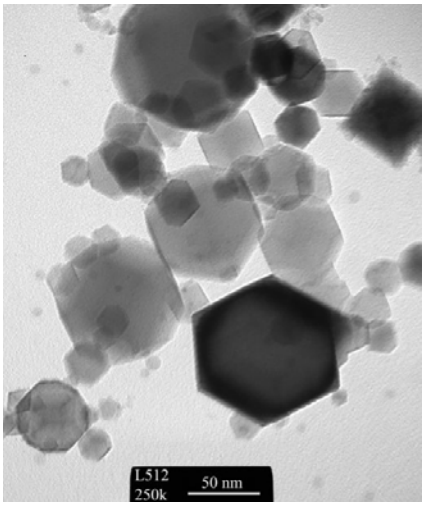

Fig. 3 TEM micrograph of product NZP2

No direct correlation was found between d_{50}(l) and saturation magnetization. However, as it was referred previously, decrease of the particle size below a given limit facilitates formation of inverse spinels. In our case it would require a much higher cooling rate of gaseous and solid species below the plasma flame region.
Similarly to the specific energy of processing, the injection position of precursors most probably also has an effect on the thermal history of precursors and products,

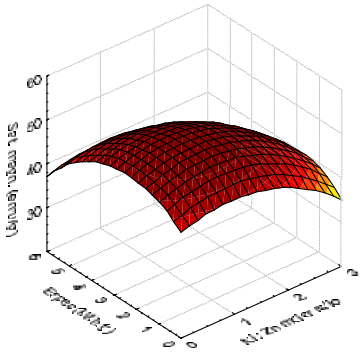

Fig. 4 Saturation magnetization as plotted against Ni:Zn molar ratio and specific energy

respectively, and thus, the particle size and saturation magnetization of ferrite powders. Further experiments have to be performed to study this effect.
The XRD patterns of ferrite powders produced in RF thermal plasma conditions (Fig. 5) confirm formation of well crystallized spinels.

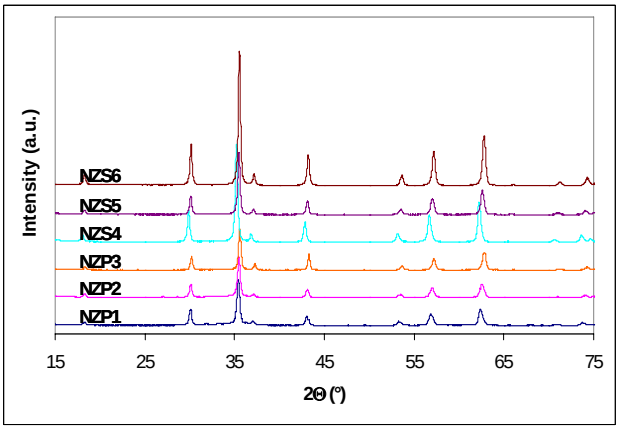

Fig. 5 XRD patterns of nickel-zinc ferrites. For legends see Table 1.

The domain sizes were calculated from the broadening of the relevant lines of X-ray diffractograms. In this series of experiments the domain size of ferrite spinels varied in the range of 18 to 50 nm (Table 1). Comparison of these data with those of particle size analyses refer to some agglomeration of primary grains in particular conditions on the one hand, and formation of intra-granular phase boundaries on the other. Agglomeration of smaller particles can be observed in Fig. 2, as well.
According to EDS measurements, there was some segregation of zinc and iron in particles of different sizes (Table 2). Some excess of Zn was detected in the smaller particles and certain excess of Fe in bigger ones. Particles of targeted composition ($Ni_{0.75}Zn_{0.25}Fe_2$) have mean particle size of 60-80 nm.

Table 2 Results of EDS measurements

Estimated mean particle size (nm)	Calculated ratio of metals
10	$Ni_{0.8}ZnFe_2$
15	$Ni_{0.84}Zn_{0.78}Fe_2$
30	$Ni_{0.72}Zn_{0.51}Fe_2$
40	$Ni_{0.78}Zn_{0.39}Fe_2$
50	$Ni_{0.7}Zn_{0.29}Fe_2$
180	$Ni_{0.82}Zn_{0.14}Fe_2$
200	$Ni_{0.78}Zn_{0.12}Fe_2$

Conclusions

It has been proved that nanosized, normal and inverse zinc ferrite spinels could be produced in a radiofrequency thermal plasma reactor from mixtures of constituting oxides and corresponding nitrate salts, respectively. Some differences were observed between the two precursors in terms of processing and also in properties of products. Composition and feed rate of precursors and the plate power of RF generator influenced the characteristic particle size and the saturation magnetization ferrite powders, as well. According to EDS measurements, zinc and iron was more or less segregated in the ferrite particles.

Acknowledgement

This work was supported by the Hungarian Scientific Research Fund (OTKA), Grant No. T047360 and the GVOP project No. 3.1.1-2004-05-0031/3.0.

References

1. T. Tsutaoka: Frequency Dispersion of Complex Permeability in Mn-Zn and Ni-Zn Spinel Ferrites and their Composite Materials - J. Appl. Phys. **93** (2003) 2789.
2. S. A. Morrison, Ch. L. Cahill, E. E. Carpenter, S. Calvin, R. Swaminathan, M. E. McHenry and V. G. Harris: Magnetic and Structural Properties of Nickel Zinc Ferrite Nanoparticles Synthesized at Room Temperature - J. Appl. Phys., **95** (2004) 6392.
3. A. Cabanas and M. Poliakoff: The Continuous Hydrothermal Synthesis of Nano-particulate Ferrites in Near Critical and Supercritical Water - J. Mater. Chem. **11** (2001) 1408.
4. P. C. Fannin, S. W. Charles, and J. L. Dormann, Field Dependence of the Dynamic Properties of Colloidal Suspensions of $Mn_{0.66}Zn_{0.34}Fe_2O_4$ and $Ni_{0.5}Zn_{0.5}Fe_2O_4$ Particles - J. Magn. Magn. Mater. **201** (1999) 98.
5. P. Druska, U. Steinike and V. Sepelák: Surface Structure of Mechanically Activated and of Mechanosynthesized Zinc Ferrite - Journal of Solid State Chemistry **146** (1999) 13.
6. G. Economos: Magnetic Ceramics I. General Methods of Magnetic Ferrite Preparation – J. Amer. Ceram. Soc. **38** (1955) 241.
7. I. Mohai, L. Gál, J. Szépvölgyi, J. Gubicza, Zs. Farkas: Synthesis of Nanosized Zinc Ferrites from Liquid Precursors in RF Thermal Plasma Reactor – J. Europ. Ceram. Soc. **27** (2007) 941.
8. I. Mészáros: Micromagnetic Measurements and their Applications - Materials Science Forum **414** (2003) 275.